International Journal of Technology

http://ijtech.eng.ui.ac.id

Research Article

Tri-Polymer-Based Injectable Hydrogel with Hybrid Crosslinking Network: Carboxymethyl Cellulose, Sodium Alginate, and Chitosan

Ayla Annisa Liswani[1], Apriliana Cahya Khayrani[1,2,3*], Ibnu Maulana Hidayatullah[1,2,3], Retno Wahyu Nurhayati[1,2,4], Sunarso Sunarso[5], Heri Setiawan[6], Hafizah Mahmud[7]

[1]Department of Chemical Engineering, Faculty of Engineering, Universitas Indonesia, Depok, 16424, Indonesia

[2]Research Center for Biomass Valorizations, Universitas Indonesia, Depok, 16424, Indonesia

[3]Research Center for Biomedical Engineering, Universitas Indonesia, Depok, 16424, Indonesia

[4]Stem Cells and Tissue Engineering Research Cluster, Indonesian Medical Education and Research Institute 11 (IMERI), Faculty of Medicine, Universitas Indonesia, Central Jakarta 10430, Indonesia

[5]Department of Dental Materials Science, Faculty of Dentistry, Universitas Indonesia, Jakarta, 10430, Indonesia

[6]Laboratory of Pharmacology, Faculty of Pharmacy, Universitas Indonesia, Depok 16424, Indonesia

[7]UTM-MPRC Institute for Oil & Gas (IFOG), Universiti Teknologi Malaysia, Skudai, Johor, 81310, Malaysia

*Corresponding author: apriliana.cahya@ui.ac.id; Tel.: +62-21-7863516; Fax.: +62-21-7863516

Abstract: Injectable hydrogel is a very promising biomaterial application in the biomedical field, especially for minimally invasive therapeutic applications due to its ability to be injected in liquid or semi-liquid form and undergo in situ gelation at the target site. Hydrogel technology based on natural multi-biopolymers such as carboxymethyl cellulose (CMC), sodium alginate (SA), and chitosan (CS) is increasingly attracting attention due to its biocompatibility, biodegradability, and biological activity that support the healing process. The use of calcium chloride ($CaCl_2$) as an ionic crosslinker allows the formation of a stable and strong gel through ionic interactions with carboxylate groups in alginate, allowing the hydrogel to have optimal mechanical and physical properties for clinical applications. In this study, a stepwise factorial experimental design was used to develop an injectable hydrogel formulation based on a combination of CMC, SA, and CS with CaCl as a crosslinker. The swelling, degradation, injectability, rheological properties, and surface morphology were characterized using scanning electron microscopy (SEM). The composition of CMC-SA-CS with a concentration of 3%:2%:2% produced the best results with a gelation time of 7.80±0.18 seconds, controlled degradation 34.01±2.33%, low swelling% of 14.90±0.08%, injectability of 87.09±0.72%, and stability expressed by a high elastic modulus (G') of 46,2 kPa. This study contributes significantly to the development of injectable biomaterials that are applicable and efficient for minimally invasive therapy, thereby opening up opportunities for the development of safer and more effective therapies.

Keywords: Carboxymethyl cellulose; Calcium chloride; Chitosan; Injectable hydrogel; Sodium alginate

1. Introduction

In the last five years, the development of biomaterial technology in the biomedical field has continued to experience significant acceleration, especially in the development of hydrogels. Hydrogels are hydrophilic polymers with a three-dimensional structure that resembles the soft tissues of the human body, making them ideal for biomedical applications (C. Zhao et al., 2022). However, conventional hydrogels still face major obstacles in clinical applications, especially the need for open surgical procedures for insertion, which increases the risk of infection. Injectable hydrogel technology has been developed with hydrogels that can be injected and undergo in

https://doi.org/10.14716/ijtech.v17i2.8202
Received November 2025; Revised November 2025; Accepted December 2025

situ gelation at the target site. Injectable hydrogel technology has the advantage of enabling minimally invasive treatment procedures (Highley et al., 2016). Their applicability spans deep in wound therapy, cartilage and bone regeneration, and localized therapeutic release (Kumar et al., 2023).

Biopolymers such as carboxymethyl cellulose (CMC), sodium alginate (SA), and chitosan (CS) are widely used as the base material for injectable hydrogels due to their advantages in biocompatibility and biodegradability. CMC is an anionic polysaccharide biocompatible with hydrophobic methyl groups, and is widely used as a biomaterial in the fields of tissue engineering, wound dressing, and drug delivery (Gaharwar et al., 2014). SA, derived from brown algae, is a natural non-toxic anionic polymer known for its ability to form stable hydrogels through ionic interactions with divalent ions, especially calcium (Ca^{2+}) (Pangesty et al., 2025; Silva et al., 2024). SA also exhibits good biocompatibility, high water absorption, facile drug delivery, and easy gel formation. By combining the biocompatibility of SA with the hydrogels' high water absorption capacity, SA-based hydrogels form materials with high application potential. These hydrogels exhibit various functions, such as environmental responsiveness, self-healing ability, and favorable mechanical properties (Wang et al., 2025). Conversely, CS is a cationic polymer with multifunctional advantages in the biomedical field and is the second most abundant polysaccharide after cellulose (Abourehab et al., 2022; Timotius et al., 2022). The complex network structure of chitosan-based hydrogels provides a versatile platform for incorporating various bioactive compounds, enabling a wide range of applications in tissue engineering, drug encapsulation, food science, and other fields. These hydrogels have demonstrated great potential in multiple fields with the ability to swell or contract in response to external stimuli (C. Zhao et al., 2022). Chitosan-based hydrogels have emerged as a promising alternative to conventional biodegradable materials due to the growing prominence of green chemistry and the urgent need for environmental preservation (Li et al., 2023).

However, hydrogels that are only based on polymers independently often have mechanical strength limitations and less than optimal gel stability. Developments were carried out by combining several polymers to overcome these challenges while improving the performance of injectable hydrogels. In the manufacture of injectable hydrogels, crosslinker agents are used to connect polymer chains to form a stable three-dimensional network (Malektaj et al., 2023). $CaCl_2$ (calcium chloride) is the most commonly used crosslinker that provides calcium ions (Ca^{2+}) that can bond ionically with carboxylate groups ($-COO^-$). Beyond alginate interactions, Ca^{2+} can influence the electrostatic balance within mixed anionic–cationic systems, contributing to network stiffness and stability while preserving suitability for biomedical environments. Injectable hydrogels utilizing $CaCl_2$ crosslinking have demonstrated relevance in bone defect filling, periodontal pocket sealing, cartilage repair, localized drug depot formation, and other applications that require rapid gel formation and structural integrity under physiological conditions (Abourehab et al., 2022). Alberts et al., 2025 synthesized a hydrogel combination of cellulose polymers with high biocompatibility and water absorption capacity for wound dressing applications. Z. Zhang and Qiao, 2021 synthesized a CMC-based hydrogel with the influence of calcium ions (Ca^{2+}) from $CaCl_2$, resulting in a significant increase in hydrogel strength. Wang et al., 2024 developed a hydrogel from a combination of SA and CS, producing a hydrogel with characteristics that support tissue regeneration therapy applications. Nevertheless, a tri-polymer injectable hydrogel combining CMC, SA, and CS within a single crosslinked network has not been systematically evaluated.

Given the limitations of single-polymer hydrogels and the lack of studies examining tri-polymer synergy, this research aims to develop and characterize an injectable hydrogel based on CMC-SA-CS polymers crosslinked with $CaCl_2$. The objective of this study is to evaluate the influence of polymer concentration variations on gelation behavior, swelling capacity, injectability, degradation profile, viscoelastic strength, and microstructural morphology. The working hypothesis is that the integration of three complementary biopolymers will produce improved gelation control, enhanced mechanical stability, and tunable degradation behavior that cannot

be achieved through single- or dual-polymer formulations. This work provides a foundational insight into the design of IHs with performance characteristics aligned to clinical biomedical applications.

2. Methods

In this study, CMC (Sigma-Aldrich, USA) with Degree of Substitution (DS) 80-95% and viscocity of 2500-6000 centi poise (in 1% H2O), SA (Sigma-Aldrich, USA) with viscocity 5.0-40.0 centi poise (in 1% H2O), CS (Bio Chitosan, Indonesia) with a medium MW and a DD of 89.5%, and $CaCl_2$ (Merck, USA) were utilized as the primary materials for hydrogel synthesis. CMC and SA served as anionic polysaccharides, providing viscosity and gel-forming capabilities, while CS, a cationic biopolymer derived from chitin, contributed to structural integrity and bioactivity. $CaCl_2$ was employed as the ionic crosslinking agent to facilitate the gelation of the hydrogel network, particularly through interactions with alginate. All materials were used without further purification, and their selection was based on biocompatibility, availability, and previous evidence of suitability in hydrogel-based biomedical applications. Because this study focuses on early-stage material formulation and physicochemical characterization, no sterilization procedure was applied. Future stages of this research could involve cytocompatibility or biomedical testing that will incorporate appropriate sterilization methods depending on polymer sensitivity.

2.1 Synthesis of the CMC-SA-CS Hydrogel

The hydrogel solution is prepared by mixing CMC, SA, and CS with a mixing ratio of 1:1:1. The experimental design in this process uses variations in the concentration of each mixture with the 23 Full Factorial Design (FFD) model. The formula design for making hydrogel was carried out with variations in the concentration of each polymer into several groups of two-level factorial designs consisting of maximum (+1) and minimum (-1) values. The variations used were 1% and 2% for the first, 2% and 3% for the second, and 1% and 3% for the third. Table 1 shows the experimental design. Chitosan solution was dissolved in acetic acid and used without pH adjustment. The resulting acidic condition was acknowledged as a factor influencing the polyelectrolyte interactions.

Table 1 Experimental design of the concentration variation

Model	Sample	CMC (%)	SA (%)	CS (%)	Model	Sample	CMC (%)	SA (%)	CS (%)	Model	Sample	CMC (%)	SA (%)	CS (%)
1	1	1	1	1	2	1	2	2	2	3	1	1	1	1
	2	2	1	1		2	3	2	2		2	3	1	1
	3	1	2	1		3	2	3	2		3	1	3	1
	4	2	2	1		4	3	3	2		4	3	3	1
	5	1	1	2		5	2	2	3		5	1	1	3
	6	2	1	2		6	3	2	3		6	3	1	3
	7	1	2	2		7	2	3	3		7	1	3	3
	8	2	2	2		8	3	3	3		8	3	3	3

CMC and SA were mixed first and then mixed with CS to avoid any unwanted initial precipitation or gelation before crosslinking. The mixing process was done using a homogenizer at a speed of 400 rpm at room temperature for 30 minutes (Possolli et al., 2024). The hydrogel solution was then poured into a well-plate 24s with a volume of 1 mL for each sample. The hydrogel formation process was carried out in a well-plate by dripping 0.5 mL of 5% $CaCl_2$ into each sample. The well plate was then placed in an incubator at 37°C until the hydrogel was completely formed. The illustration of the preparation of the CMC–SA–CS hydrogel is shown in Figure 1.

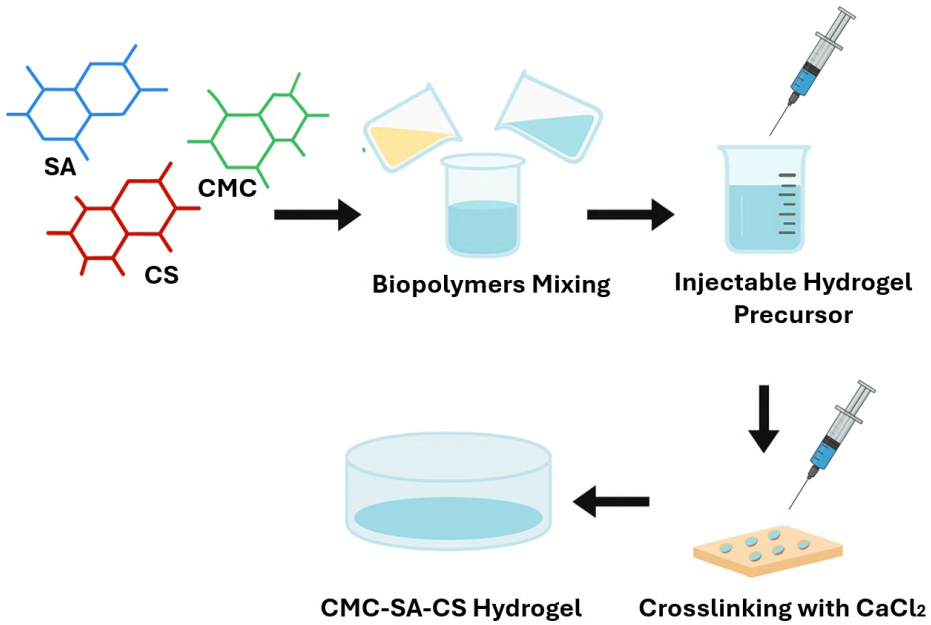

Figure 1 CMC-SA-CS Hydrogel Synthesis Workflow

2.2 Injectability test

The injectability test was conducted using a 21G syringe to see the ability of the hydrogel to be injected from a syringe. This was done by injecting the hydrogel into a Petri dish. The Petri dish containing the hydrogel was then weighed, and the percentage of injectability was calculated (Amanda et al., 2022; Alonso et al., 2021) using Equation (1).

$$\text{Injectability}(\%) = \frac{\text{Mass extruded from syringe}}{\text{Total mass before injection}} \times 100 \tag{1}$$

2.3 Gelation time

The gelation time was determined using an inverted tube test. The hydrogel was placed in a 1 mL vial and then dripped with 0.5 mL of 5% $CaCl_2$. The vial was then inverted at certain time intervals to observe gelation time. The gelation time was defined as the time when the gel did not flow out (Fattahpour et al., 2020).

2.4 Swelling test results

The dried hydrogel samples were weighed accurately using a digital scale and then immersed in phosphate-buffered saline (PBS) (Gibco, New York) in a well-plate at 37 °C for 2 h. Furthermore, every 30 min, the samples were removed from the PBS solution, and the excess solution on the surface was removed using tissue paper. The samples were then weighed accurately (Fattahpour et al., 2020). The swelling ratio was then calculated to determine the water absorption capacity of the hydrogel using Equation (2), where W_s is the weight of the swollen hydrogel sample, and W_d is the dry weight of the hydrogel sample.

$$\text{Swelling ratio}(\%) = \frac{(W_s - W_d)}{W_d} \times 100 \tag{2}$$

2.5 In vitro degradation test

The dried hydrogel samples were immersed in 50 mL of phosphate-buffered saline solution at 37°C. After 2 h, the samples were removed, and the excess solution on the surface was removed using filter paper. Subsequently, the samples were returned to the medium, and the

above process was repeated. The PBS medium was replaced with a new one every 3 days to prevent microbial contamination and volume reduction. Weight loss over time was considered degradation, and the remaining weight of the hydrogel was re-dried and calculated as the final weight (Fattahpour et al., 2020). The degradation rate was calculated using Equation (3), where W_2 is the weight of the swollen hydrogel after 2 h of incubation in PBS solution, and W_t is the weight of the swollen hydrogel after the degradation period.

$$\text{Degradation}(\%) = \frac{W_t}{W_2} \times 100 \tag{3}$$

2.6 Rheology

A rheology test was conducted to determine the resistance and stability properties of the resulting hydrogel, the results of which were expressed as elastic modulus (G') and viscous modulus (G''). This test was conducted using a Discovery Hybrid Rheometer (DHR10) at the Integrated Laboratory and Research Center (ILRC) at the University of Indonesia. The hydrogel sample was gently loaded onto the lower plate, and the plate gap was automatically adjusted using the standard auto-trim and set-gap procedure to ensure uniform contact between the plates. The excess sample was trimmed before testing. A strain sweep (0.01–1000% strain, 10 rad/s) was conducted to determine the Linear Viscoelastic Region (LVE).

2.7 Scanning Electron Microscopy (SEM)

SEM test was conducted as a qualitative analysis of the hydrogel produced to observe its porous microstructure. Samples were freeze-dried for 17 h and sputter-coated with gold to avoid surface charging during scanning electron microscopy (SEM) imaging. The test results are 3D images of the sample surface, which display structural details down to the nanometer scale. This test was conducted at the Department of Electrical Engineering, UP2M Laboratory, University of Indonesia.

2.8 Statistical analysis of the data

All results are presented as the mean ± standard deviation (SD). Statistical analysis was performed using GraphPad Prism® to evaluate differences within formulations. Statistical significance was determined based on p-values, with thresholds set at $p \leq 0.05$ (*), $p \leq 0.01$ (**), $p \leq 0.001$ (***), and $p \leq 0.0001$ (****).

3. Results and Discussion

3.1 Synthesis of the CMC-SA-CS Hydrogel

Each formulation of models 1, 2, and 3 was contacted with 5% $CaCl_2$, and the changes that occurred in the CMC-SA-CS polymer solution were observed. The formation of the CMC–SA–CS hydrogel proceeds through a sequential and cooperative assembly process driven by Ca^{2+} crosslinking, polyelectrolyte complexation, and hydrogen bonding. When $CaCl_2$ is introduced into the polymer mixture, the first and most dominant event is the ionic crosslinking of sodium alginate by Ca^{2+}, which follows the classical egg-box model. In this mechanism, Ca^{2+} ions selectively bind to the guluronate (G-block) regions of alginate through coordination with carboxylate groups ($–COO^-$), forming bidentate ionic bridges that create stable junction zones within the hydrogel network. This rapid ionic coordination is widely recognized as the primary determinant of SA gel stiffness and 3D network formation (Makarova et al., 2023). CS bears protonated amine groups ($–NH_3^+$), which exhibit strong attraction to the negatively charged carboxylate moieties on SA and CMC (Baysal et al., 2013). This attraction leads to the formation of polyelectrolyte complexes that tighten and densify the partially crosslinked matrix, especially in the regions where alginate chains remain insufficiently coordinated by Ca^{2+}. Hy-

drogen bonding is another structural contribution facilitated by the hydroxyl-rich backbone of CMC and the amine and hydroxyl groups of CS. This bonding can occur both within and between polymer chains CMC and CS, or CMC and SA, resulting in additional physical crosslinks that enhance elasticity, cohesive strength, and water retention (H. Zhao et al., 2025). Figure 2 illustrates the mechanism of CMC-CS-SA interactions.

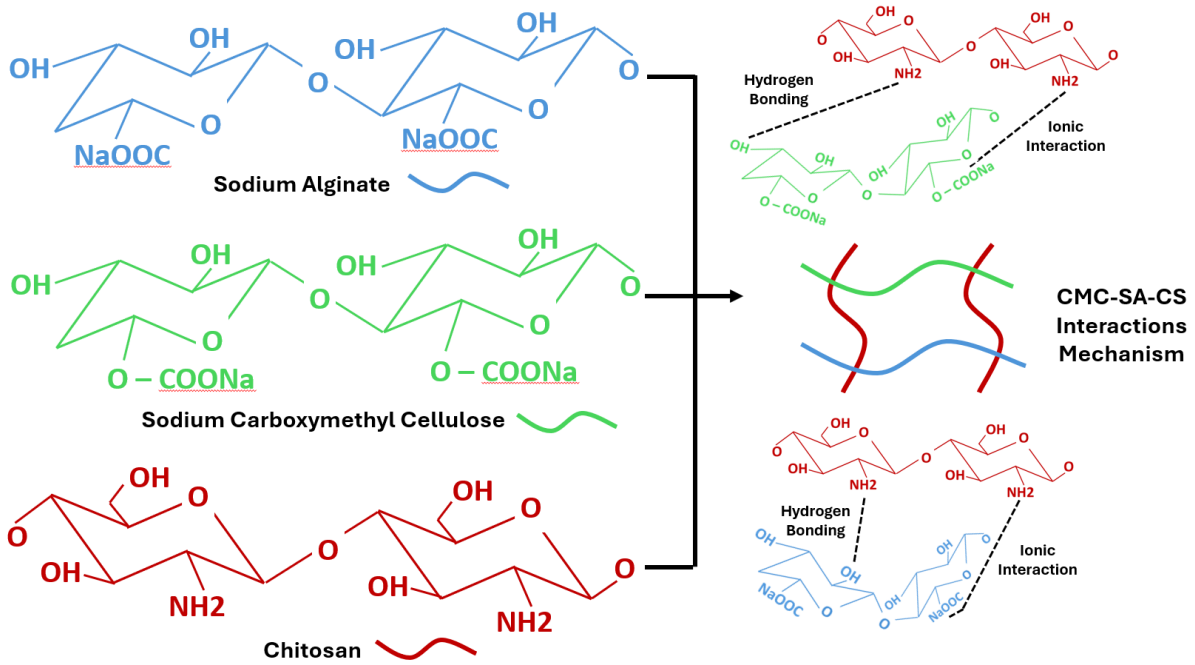

Figure 2 CMC-SA-CS Interactions Mechanism

As shown in Table 2, hydrogel formation in model 1 occurred successfully in formulations 1:2:2 and 2:2:2, whereas the hydrogel did not form completely for other formulations in this model, resulting in a fragile and non-rigid mixture. This phenomenon can occur because at low SA concentrations, it does not provide enough hydroxyl groups to interact with Ca^{2+}, where SA is more effective in binding to Ca^{2+}, ions than CMC because SA has a G-block that can form an egg box structure. In the 2^{nd} model, stable hydrogels were successfully formed in all formulation variations. This shows that at concentrations of 2 % and 3%, each polymer is already at a sufficient threshold to form a stable crosslink network. Meanwhile, for the 3rd model, the hydrogel formed was only in five

%CMC:%SA:%CS formulations. In addition, low polymer concentrations produced inadequate chain entanglement and insufficient network density, reinforcing the dependence of gel formation on both ionic and physical interactions. Although the initial mixing of CMC, SA, and chitosan allows early polyelectrolyte interactions between protonated chitosan ($–NH_3^+$) and the carboxylate groups ($– COO^-$) of SA and CMC to form, these interactions do not dominate the final hydrogel structure. Once $CaCl_2$ is introduced, Ca^{2+} exhibits a much stronger and more specific affinity to SA carboxylates and rapidly forms egg-box junction zones. As a result, Ca^{2+},-SA crosslinking becomes the primary structural mechanism, whereas the electrostatic binding of CS remains only in polymer-dense regions where Ca^{2+} diffusion is limited. Thus, the interactions and hydrogen bonding among CMC, SA, and CS act as secondary reinforcement that enhances network compactness but does not supersede the dominant Ca^{2+} crosslinking. This competitive yet cooperative mechanism explains the observed differences in gelation behavior. Table 2 shows that 15 formulations can be continued to the characterization process to determine both the physical and chemical properties of the CMC- SA-CS hydrogel crosslinked with 5% $CaCl_2$.

Table 2 Evaluation of hydrogel formation

Model					
1		2		3	
Formulation (%CMC:%SA:%CS)	Formation of hydrogel	Formulation (%CMC:%SA:%CS)	Formation of hydrogel	Formulation (%CMC:%SA:%CS)	Formation of hydrogel
1:1:1	Not formed	2:2:2	Formed	1:1:1	Not formed
2:1:1	Not formed	3:2:2	Formed	3:1:1	Not formed
1:2:1	Not formed	2:3:2	Formed	1:3:1	Formed
2:2:1	Not formed	3:3:2	Formed	3:3:1	Formed
1:1:2	Not formed	2:2:3	Formed	1:1:3	Formed
2:1:2	Not formed	3:2:3	Formed	3:1:3	Not formed
1:2:2	Formed	2:3:3	Formed	1:3:3	Formed
2:2:2	Formed	3:3:3	Formed	3:3:3	Formed

3.2 Injectability

Injectability is a crucial parameter in situ hydrogel development that is used to determine the ability and ease of releasing the hydrogel through a syringe. The testing was performed on a hydrogel precursor solution, (before Ca^{2+} addition) because its viscosity reflects the actual conditions when the precursor is still in liquid form when the material is injected into the body. This test also ensures that the precursor can flow when pressure is applied but immediately gels when it meets Ca^{2+} ions in the target tissue (Parvin et al., 2025). After Ca^{2+} is added, a rapid gelation process occurs through ionic cross-linking, causing the viscosity to increase drastically so that the material is no longer injectable. The results of the injectability test are shown in Table 3, where the highest injectability was achieved by formulation 1%:2%:2% with an injectability value of 90.91±1.79%, with significancy of each formulation shown in Figure 3. This is in accordance with the theory that CMC at low to moderate concentrations provides a lubricating effect and increases precursor fluid, while SA and CS in moderate amounts are insufficient to significantly increase viscosity (Zamini et al., 2025). These injectability results are in accordance with the shear thinning hydrogel concept: the higher the initial viscosity, the greater the pressure required (Yang et al., 2023). Overall, a negative correlation was found between the total polymer concentration and precursor injectability, whereas the higher the polymer, the lower the injectability. The optimal formulation is one with an injectability above 85% (1:2:2, 2:3:2, 2:2:3), as these findings align with syringe-based delivery requirements and emphasize the importance of balancing viscosity and polymer loading for clinical usability.

3.3 Gelation time

The gelation time measurement mechanism is performed using the inverted vial method. The gelation time calculation begins when the CMC-SA-CS mixture solution is dripped by a 5% $CaCl_2$ crosslinker. The gelation time is an important parameter in the development of hydrogels, especially for in situ forming applications or injection systems. Based on Table 2, only gelation occurred in 15 formulations. The gelation time results of each formulation with a total of 15 formulations are shown in Table 4. Gelation time is calculated until the hydrogel no longer moves or flows, indicating that gelation has occurred. Gelation time measurements were performed in duplicate, and the average value of the measurement data is attached. The gelation

time measurements of 15 variations of CMC-SA-CS formulations using the vial inverting method showed that the polymer concentration ratio greatly affected the hydrogel formation speed after the addition of 5% $CaCl_2$. The significancy of each formulation in gelation time shown in Figure 4.

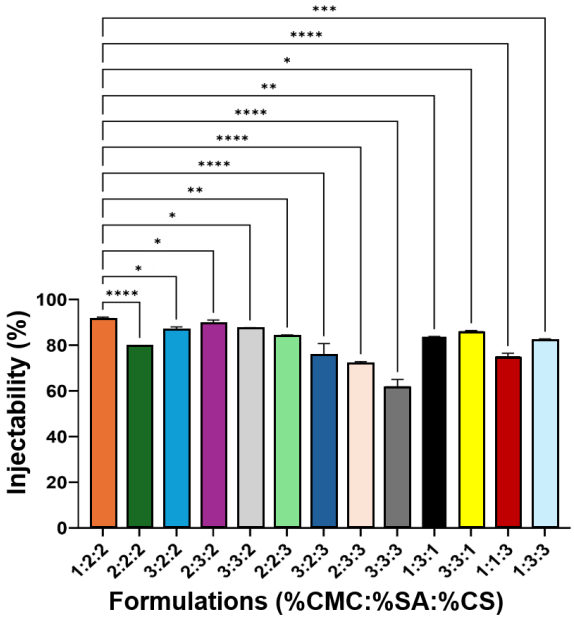

Figure 3 Statistical significance is expressed as mean ± SD. Multiple comparisons were evaluated with significance levels indicated as * ($p < 0.05$), (**) ($p < 0.005$), (***) ($p < 0.001$), and (****) ($p < 0.0001$).

Table 3 Injectability of the CMC-SA-CS precursor solution

Model	Formulation (%CMC : %SA : %CS)	Injectability (%)
	1:2:2	90.91±1.79
	2:2:2	85.03±0.83
1	2:2:2	85.03±0.83
	3:2:2	86.99±0.91
	2:3:2	89.54±1.54
	3:3:2	87.09±0.72
	2:2:3	88.49±0.06
2	3:2:3	85.28±2.85
	2:3:3	72.25±0.56
	3:3:3	61.54±2.20
	1:3:1	83.67±0.14
	3:3:1	85.67±0.96
3	1:1:3	75.19±1.29
	1:3:3	83.58±0.16
	3:3:3	61.54±2.20

In general, formulations with high SA concentrations exhibited fast gelation times. Formulations 2:3:2 and 3:3:2 showed gelation times of 9.41 and 7.80 s, respectively, which were the fastest among all samples. This is in line with the theory that increasing alginate concentration will increase the number of carboxylate groups (COO^-) that can interact with Ca^{2+} ions, forming stable "egg-box" cross-links and accelerating gel formation (Savić Gajić et al., 2023). Gelation under 10 s may increase the risk of needle clogging. Thus, practical delivery strategies,

such as dual-barrel syringe systems or mixing at the defect site, are recommended. Formulations such as 1:3:1 and 1:2:2 had the longest gelation times (29.03 and 25.96 s), respectively, indicating that the number of available COO^- groups was very limited and the crosslinking process was slow.

Table 4 Gelation time of the injected hydrogel

Model	Formulation (%CMC : %SA : %CS)	Gelation Time (second)
	1:2:2	25.96±0.16
	2:2:2	16.73±0.05
1	2:2:2	16.73±0.05
	3:2:2	12.82±0.28
	2:3:2	9.41±0.042
	3:3:2	7.80±0.18
	2:2:3	14.08±0.18
2	3:2:3	16.27±0.18
	2:3:3	10.99±0.22
	3:3:3	21.42±0.83
	1:3:1	29.03±0.078
	3:3:1	21.74±0.88
3	1:1:3	21.20±0.60
	1:3:3	23.29±0.48
	3:3:3	25.96±0.16

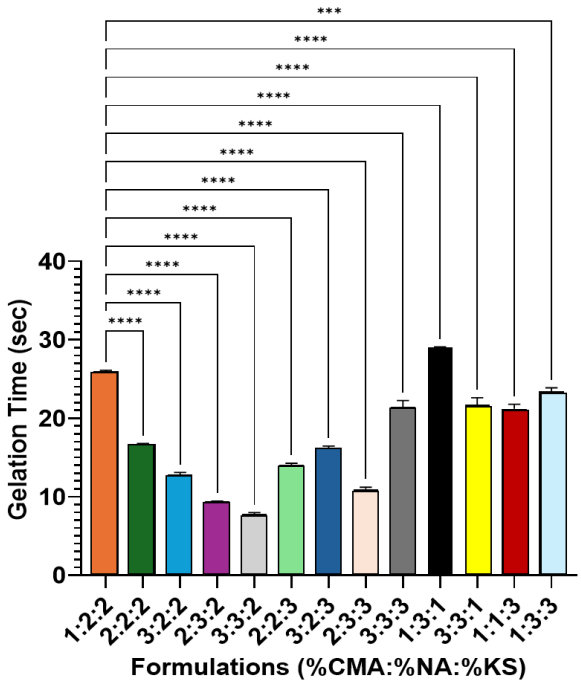

Figure 4 Statistical significance of gelation time is presented as mean ± SD followed by multiple comparisons, with (*) indicating $p < 0.001$ and (**) indicating $p < 0.0001$.

3.4 Swelling test results

A swelling test was conducted to assess the fluid absorption ability of the hydrogel, a key indicator of its capacity to maintain moisture. The%CMC:%SA:%CS ratio showed a significant influence on swelling across all three models as shown in Figure 5. In Model 1, swelling decreased

with higher chitosan content, as stronger electrostatic interactions between -COO^- (CMC/AA) and -NH_3^+ (CS) increased crosslink density and reduced porosity [19]. In Model 2, the 3:2:3 formulation

showed the highest swelling (20%), attributed to abundant hydrophilic -OH and -COO^- groups from CMC (Savić Gajić et al., 2023), whereas excessive chitosan in 2:3:3 and 3:3:3 reduced swelling due to over-crosslinking that limited water diffusion (Feyissa et al., 2023). The optimized formulation (3:2:2) exhibited the lowest swelling (14.90 ± 0.08%), indicating a dense network favorable for load-bearing biomedical settings. The extended swelling time further revealed a decline after 150 min, indicating that structural stability eventually outweighs water uptake.

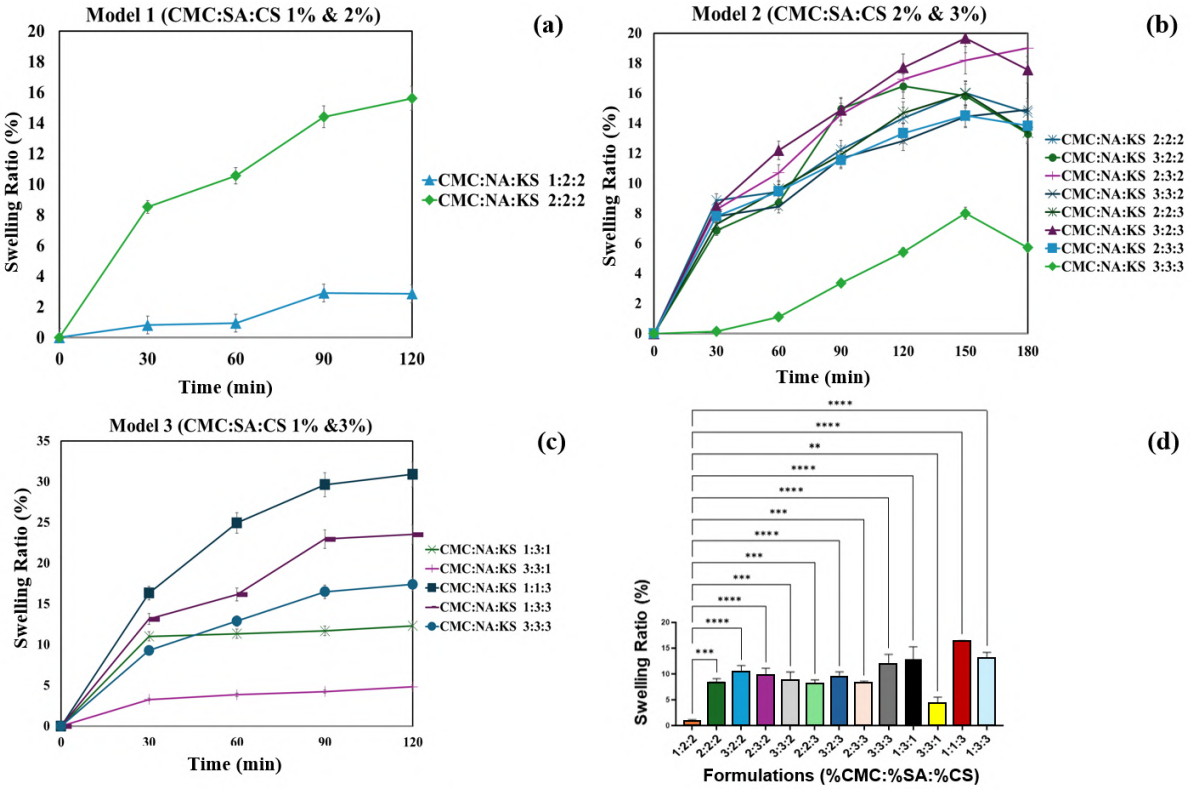

Figure 5 Swelling ratio in Models (a)1, (b)2, (c)3, and (d) statistical significance of Swelling Ratio 300 presented as mean ± SD followed by multiple comparisons, with (*) for $p < 0.005$, (**) for $p < 0.005$, (***) for $p < 0.001$ and (****) for $p < 0.0001$

3.5 In vitro degradation test

The hydrogel degradation test is an important parameter for assessing the stability and durability of materials in biological environments. In this study, degradation testing was carried out by calculating the weight of the hydrogel soaked in PBS solution for 10 days with intervals of 1, 3, 7, and 10 days. Figure 6 shows the percentage degradation graph of each formulation in each sample. The results of the degradation tests of the three models indicate that the stability of the hydrogel is greatly influenced by the concentration balance between polymer components. In Model 1, the 1:2:2 formulation degraded almost completely (>90%) on day 10, reflecting insufficient network stability due to low CMC and chitosan content, despite alginate's ionic crosslinking with Ca^{2+}. In contrast, the 2:2:2 formulation degraded more slowly (70%) on day 10, indicating that higher CMC enhanced structural stability through hydrogen bonding and higher initial viscosity. Huang (2016) reported that CMC/SA hydrogels with low ratios exhibit poor stability due to limited crosslinking. In Model 2, 2:2:2 and 3:2:2 exhibited the highest degradation (75% and 89%) at day 10, respectively, suggesting that lower

CS content and weaker polymer packing produced looser networks that degraded more readily (Silva et al., 2024). Other formulations with higher CS or different ratios degraded more slowly (<50%), consistent with CS's known resistance to enzymatic and hydrolytic degradation compared to SA and CMC (Abourehab et al., 2022). The role of $CaCl_2$ crosslinking was also evident, as tighter ionic networks slowed water penetration, reducing degradation. In Model 3, the 1:1:3 and 1:3:1 formulations degraded very rapidly (>90%) within 7 days due to the low concentrations of two out of three polymers, resulting in fragile and unbalanced networks. Specifically, 1:1:3 had insufficient CMC and SA, whereas 1:3:1 lacked adequate CMC and CS crosslinking with Ca2+. Conversely, 3:3:3 and 1:3:3 exhibited the lowest degradation (<50%) on day 10, indicating that higher SA and balanced polymer ratios promote denser, more durable gels. In summary, formulations such as 2:2:2 and 3:2:2 degraded faster, making them suitable for short-term therapeutic applications, such as controlled drug release or temporary scaffolds for tissue regeneration. Slower-degrading formulations (3:2:2) showed controlled degradation (34.01 ± 2.33%), making them suitable for applications requiring temporary structural support. The degradation profile is strongly influenced by the polymer composition. CMC enhances hydrolytic breakdown due to its hydrophilicity, high CS content reduces stability against ionic interactions, and SA contributes to network reinforcement via Ca^{2+} crosslinking. Hydrophilic surfaces are important for promoting a favorable environment for bone formation (Dewi et al., 2020). Thus, tailoring the balance among CMC, SA, and CS, along with crosslinking density, is essential for aligning hydrogel degradation with therapeutic demands (Silva et al., 2024).

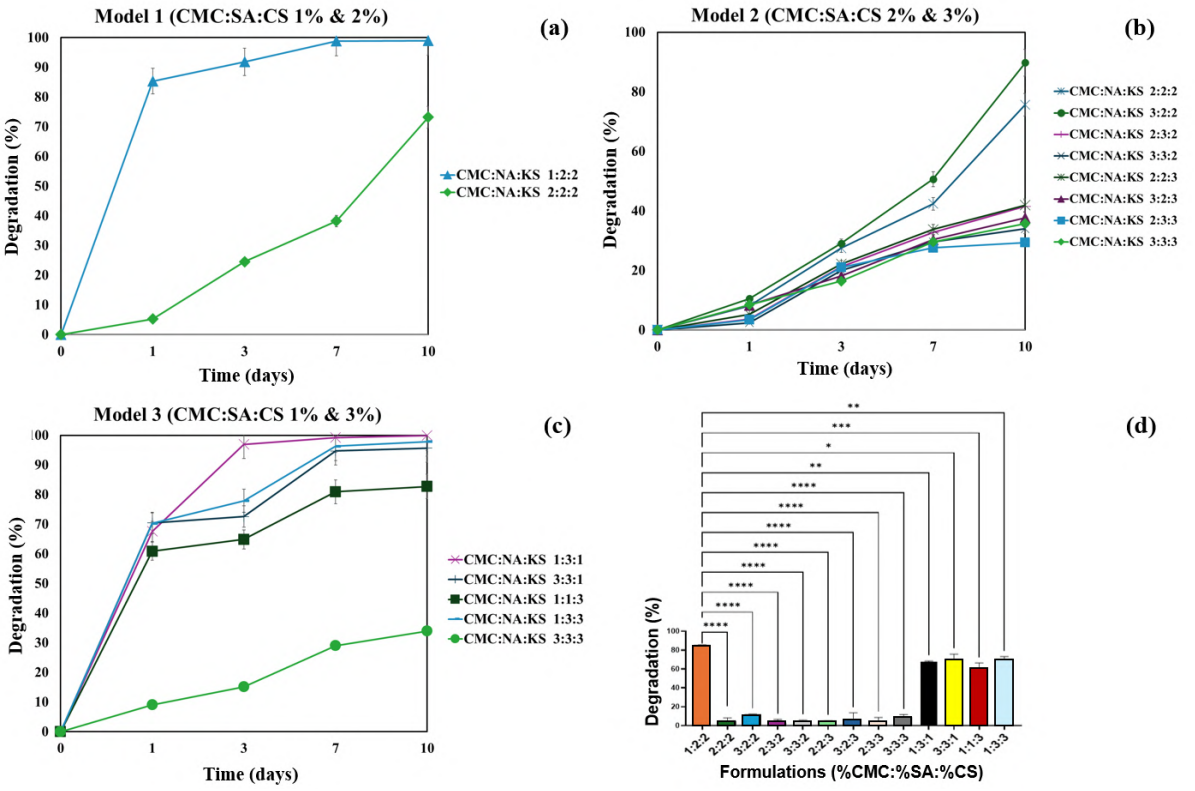

Figure 6 Degradation in Models (a)1, (b)2, (c)3, and statistical significance of 337 presented as mean ± SD followed by multiple comparison, with (*) for $p < 0.005$, (**) for $p < 0.005$, (***) for $p < 0.001$ and (****) for $p < 0.0001$

3.6 Scanning electron microscopy

SEM was used to visualize the internal microstructure before and after degradation. Both surface areas were captured, as shown in Figure 7. The pre-degradation samples show a porous network composed of interconnected polymer strands with relatively large and open pores. Such

pore structures are commonly reported in polysaccharide-based hydrogels, including CMC and SA, and are associated with high water uptake, efficient swelling, and enhanced solute diffusion (X. Zhang et al., 2021). In contrast, the post-degradation samples exhibited markedly smaller and denser pores with smoother surfaces, indicating structural compaction. This change suggests that the more weakly bound or hydrophilic segments (-OH, -COOH groups) dissolved earlier during degradation, leaving behind a tighter, reorganized network. X. Zhang et al., 2021 reported similar pore shrinkage and matrix densification during hydrogel degradation. The collapse of pores is consistent with the partial loss of crosslinks and removal of amorphous regions, resulting in reduced water-holding capacity (Franke and Gerlach, 2020). These morphological changes align with the mass-loss degradation data, where the dissolution of easily degradable polymer fractions produced both macroscopic shrinkage and microscopic densification. Collectively, SEM observations confirm that degradation progressively disrupts the pore architecture and compacts the polymer network, reducing the swelling capacity and internal diffusion pathways.

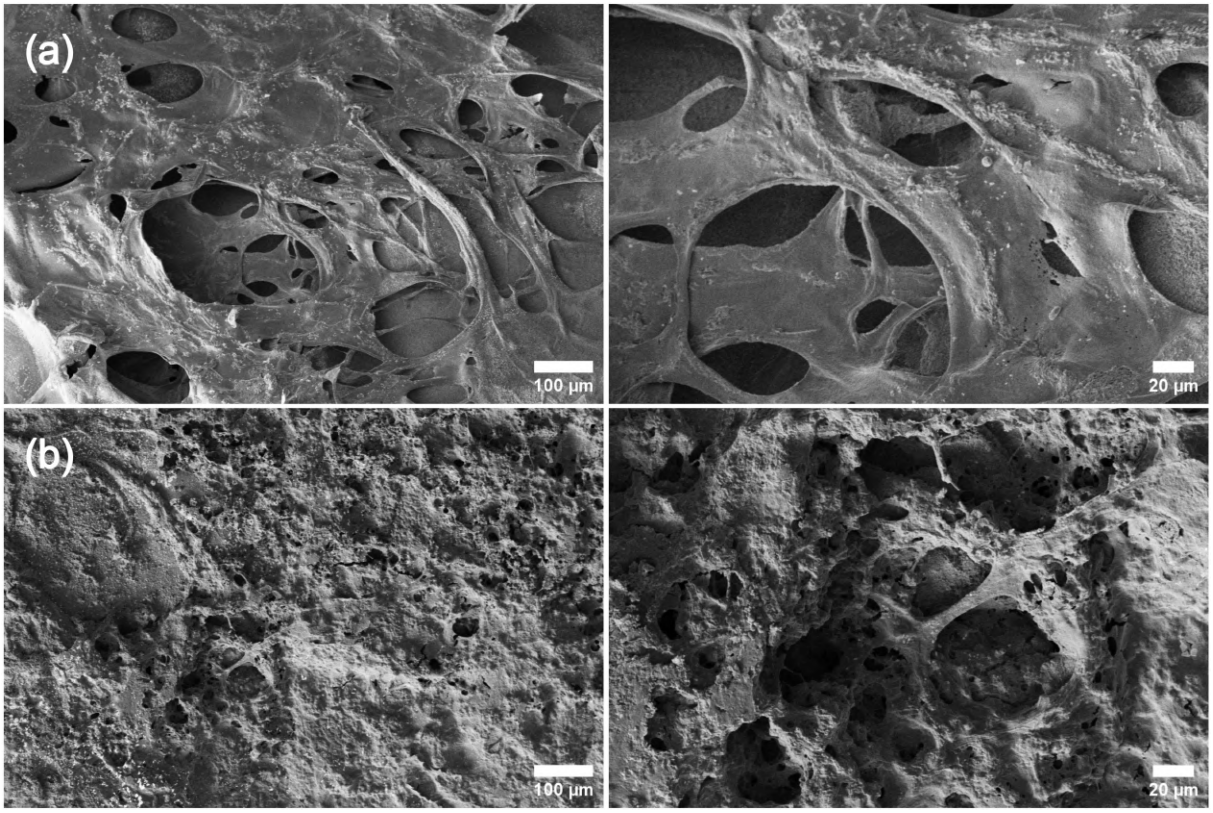

Figure 7 SEM images of the hydrogel (a) before degradation and (b) after degradation (left: scale bar 100 μm, $\times$300 magnification and right: scale bar 20 μm, $\times$1000 magnification)

3.7 Rheology

The hydrogel rheology test was conducted using a rheometer with the oscillation amplitude sweep method, where the sample was subjected to a progressively increasing oscillatory strain while maintaining a constant frequency. In the low strain range (around 10^{-2} to 10^{0} %), the G' value is consistently high, indicating that the hydrogel is in a dominant elastic state, has a strongly bound network structure, and can withstand deformation without significant energy loss. When the strain increases beyond the limits of about 10^{0} % to 10^{2} %, G' decreases, indicating that the hydrogel begins to experience structural damage or the crosslink network begins to break down (Ramli et al., 2022). The point of intersection between G' and G'' (crossover strains) at approximately 100% strain indicates the limit of viscoelastic linearity or linear viscoelastic region (LVR), after which the hydrogel exhibits predominantly viscous behavior (fluid-like) (Stojkov et al., 2021). The results of the rheological test are shown in Table 5. The rheological test

results showed that the hydrogel had good viscoelastic characteristics at low strains, but the internal network structure began to break down at strains above 100%. The 3:2:2 hydrogel composition exhibited the highest elastic modulus (46.2 kPa), indicating strong structural stability. The higher modulus indicates better load-bearing capability relevant for bone or soft-tissue support. This condition was in accordance with the characteristics of a hydrogel with structural and functional success in soft or hard tissue- based injection applications. In addition, the hydrogel rheology provided a deep understanding of the structure's resistance to mechanical forces and could be used to predict or validate the hydrogel's swelling and degradation characteristics.

Based on the rapid gelation, adequate viscoelastic strength, and controllable swelling and degradation behavior demonstrated in this study, the CMC-SA-CS hydrogel crosslinked with $CaCl_2$ shows strong potential for several minimally invasive biomedical applications as illustrated in Figure 8. The fast gelation upon Ca^{2+} exposure suggests suitability for filling bone defects, where in situ solidification is required to occupy irregular cavities and provide temporary mechanical support during early healing. The interconnected, water-rich network also enables localized drug delivery, as therapeutic molecules can be loaded into the hydrogel before injection and released gradually through diffusion or network degradation. In addition, the soft and hydrated polymer matrix, combined with its injectability, makes this formulation relevant for soft-tissue repair, including periodontal pockets, subcutaneous filler applications, or cartilage microdefects where conformal filling and gentle tissue integration are required (Li et al., 2023; X. Zhang et al., 2021; Highley et al., 2016).

Table 5 Rheology test results of CMC-SA-CS hydrogel using the Oscillation method

Formulation (%CMC : %SA : %CS)	G′ (kPa)	Strain Maximum LVR (%)	Crossover Strains (%)
1:2:2	16.23	0.40	51.34
2:2:2	22.81	0.32	25.81
3:2:2	225.87	0.79	20.66
2:3:2	16.89	0.40	64.68
3:3:2	46.20	0.40	27.34
2:2:3	15.02	0.40	41.05
3:2:3	10.93	0.63	82.52
2:3:3	38.79	0.32	23.96
3:3:3	21.73	0.50	28.64
1:3:1	30.74	0.25	30.38
3:3:1	54.78	0.20	20.87
1:1:3	15.23	0.32	25.24
1:3:3	22.29	0.25	51.29

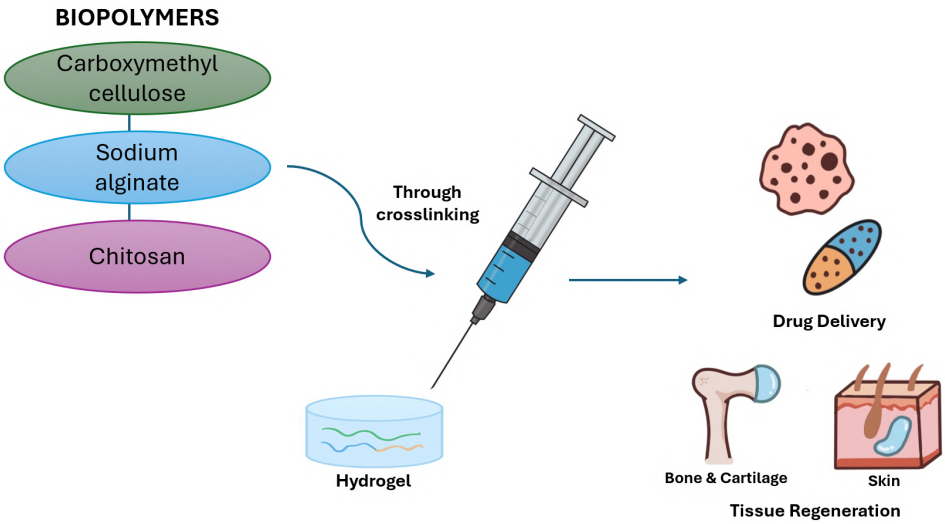

Figure 8 CMC-SA-CS Hydrogel Potential Applications

4. Conclusions

In this study, we successfully developed and characterized an injectable hydrogel system based on a tri-polymer combination of CMC, SA, and CS crosslinked using $CaCl_2$. The optimized formulation demonstrated a balanced performance characterized by rapid yet controllable gelation, adequate injectability, low swelling tendency, moderate degradation rate, and high elastic modulus, indicating its suitability for biomedical applications requiring structural integrity. The results validated that hydrogel formation is governed by three major interactions, such as Ca^{2+}-mediated egg-box crosslinking, electrostatic interactions among the polymers, and hydrogen bonding, which determine network density and stability. This work highlights the practical relevance of the developed hydrogel for minimally invasive biomedical interventions such as bone defect filling, periodontal pocket sealing, and localized drug delivery, strengthening the justification for its clinical potential. Overall, this research provides a foundational understanding of how multi-biopolymer compositions govern the functional performance of injectable hydrogels and offers a framework for further development toward clinical translation.

Acknowledgements

The authors gratefully acknowledge the financial support provided by Directorate Research and Development Universitas Indonesia funded by Q2 Scheme Research Grant (Hibah Publikasi Terindeks Internasional PUTI Q2) Grant No. NKB-1687/UN2.RST/HKP.05.00/2020 and by Direktorat Jenderal Riset dan Pengembangan Kementrian Pendidikan Tinggi, Sains, dan Teknologi with Grant No. PKS-584/UN2.RST/HKP.05.00/2025 for Penelitian Tesis Magister Scheme.

Author Contributions

AAL and ACK: Conceived designed the experiments, supervised, and wrote and finalized the draft. IMH: Methodology, formal analysis, data curation, and writing the original draft. RWN and SS: Methodology HS and HM: review and editing. AAL and ACK: Editing and finalizing the draft.

Conflict of Interest

The authors declare no conflicts of interest.

Declaration of AI

The authors declare that artificial intelligence was only used to assist in language editing and sentence refinement, not in data analysis or interpretation.

References

Abourehab, M. A. S., Pramanik, S., Abdelgawad, M. A., Abualsoud, B. M., Kadi, A., Ansari, M. J., & Deepak, A. (2022). Recent advances of chitosan formulations in biomedical applications. *International Journal of Molecular Sciences*, *23*, 10975. https://doi.org/10.3390/ijms231810975

Alberts, A., Moldoveanu, E.-T., Niculescu, A.-G., & Grumezescu, A. M. (2025). Hydrogels for wound dressings: Applications in burn treatment and chronic wound care. *Journal of Composites Science*, *9*(3), 133. https://doi.org/10.3390/jcs9030133

Alonso, J. M., Del Olmo, J. A., Gonzalez, R. P., & Saez-Martinez, V. (2021). Injectable hydrogels: From laboratory to industrialization. *Polymers*, *13*(4), 650. https://doi.org/10.3390/polym13040650

Amanda, H. G., Elline, E., & Fibryanto, E. (2022). Synthesis and physical characterization of nano-hydroxyapatite-collagen-epigallocatechin-3-gallate hydrogel composite. *Journal of Indonesian Dental Association*, *5*(1), 7. https://doi.org/10.32793/jida.v5i1.769

Baysal, K., Aroguz, A. Z., Adiguzel, Z., & Baysal, B. M. (2013). Chitosan/alginate crosslinked hydrogels: Preparation, characterization and application for cell growth purposes. *International Journal of Biological Macromolecules*, *59*, 342–348. https://doi.org/10.1016/j.ijbiomac.2013.04.073

Dewi, A. H., Yulianto, D. K., Ana, I. D., Rochmadi, & Siswomihardjo, W. (2020). Effect of cinnamaldehyde, an anti-inflammatory agent, on the surface characteristics of a Plaster of Paris–CaCO3 hydrogel for bone substitution in biomedicine. *International Journal of Technology*, *11*(5), 963–973. https://doi.org/10.14716/ijtech.v11i5.4313

Fattahpour, S., Shamanian, M., Tavakoli, N., Fathi, M., Sadeghi-Aliabadi, H., Sheykhi, S. R., & Fesharaki, M. (2020). An injectable carboxymethyl chitosan–methylcellulose–pluronic hydrogel for the encapsulation of meloxicam loaded nanoparticles. *International Journal of Biological Macromolecules*, *151*, 220–229. https://doi.org/10.1016/j.ijbiomac.2020.02.002

Feyissa, Z., Edossa, G. D., Gupta, N. K., & Negera, D. (2023). Development of double crosslinked sodium alginate/chitosan-based hydrogels for controlled release of metronidazole and its antibacterial activity. *Heliyon*, *9*, e20144. https://doi.org/10.1016/j.heliyon.2023.e20144

Franke, D., & Gerlach, G. (2020). Swelling studies of porous and nonporous semi-IPN hydrogels for sensor and actuator applications. *Micromachines*, *11*, 425. https://doi.org/10.3390/mi11040425

Gaharwar, A. K., Peppas, N. A., & Khademhosseini, A. (2014). Nanocomposite hydrogels for biomedical applications. *Biotechnology and Bioengineering*, *111*, 441–453. https://doi.org/10.1002/bit.25160

Highley, C. B., Prestwich, G. D., & Burdick, J. A. (2016). Recent advances in hyaluronic acid hydrogels for biomedical applications. *Current Opinion in Biotechnology*, *40*, 35–40. https://doi.org/10.1016/j.copbio.2016.02.008

Kumar, A., Ali, A., Kanika, Vyawahare, A., Ahmad, A., Mishra, R. K., Ansari, M. M., Nadeem, A., Siddiqui, N., Raza, S. S., & Khan, R. (2023). Highly biocompatible smart injectable hydrogel for the management of rheumatoid arthritis. *ACS Biomaterials Science & Engineering*, *9*(9), 5312–5321. https://doi.org/10.1021/acsbiomaterials.3c00514

Li, S., Mao, W., Xia, L., Wu, X., Guo, Y., Wang, J., Huang, J., Xiang, H., Jin, L., Fu, H., & Shou, Q. (2023). An injectable, self-healing and degradable hydrogel scaffold as a functional biocompatible material for tissue engineering applications. *Journal of Materials Science*, *58*, 6710–6726. https://doi.org/10.1007/s10853-023-08393-8

Makarova, A. O., Derkach, S. R., Khair, T., Kazantseva, M. A., Zuev, Y. F., & Zueva, O. S. (2023). Ion-induced polysaccharide gelation: Peculiarities of alginate egg-box association with different divalent cations. *Polymers*, *15*(5), 1243. https://doi.org/10.3390/polym15051243

Malektaj, H., Drozdov, A. D., & deClaville Christiansen, J. (2023). Mechanical properties of alginate hydrogels cross-linked with multivalent cations. *Polymers*, *15*, 3012. https://doi.org/10.3390/polym15143012

Pangesty, A. I., Kamila, R. A., Schlumbergerina, A. C. P. B., Faizurrizqi, M. D., Fakhri, R. W., Sunarso, S., Zakaria, M. N., Nuraini, L., & Azwani, W. (2025). Injectable alginate-collagen hydrogel with propolis: A potential cardioprotective biomaterial. *International Journal of Technology*, *16*(3), 1019–1029. https://doi.org/10.14716/ijtech.v16i3.7366

Parvin, N., Joo, S. W., & Mandal, T. K. (2025). Injectable biopolymer-based hydrogels: A next-generation platform for minimally invasive therapeutics. *Gels*, *11*(6), 383. https://doi.org/10.3390/gels11060383

Possolli, N. M., de Souza Niero, A. L., Modolon, H. B., da Silva Lemos, I., De Pieri, E., Machado-de-Ávila, R. A., Streck, E. L., Montedo, O. R. K., Angioletto, E., & Arcaro, S. (2024). Bioactive glass enhanced alginate/carboxymethyl cellulose functional dressings Li2O–ZrO2–SiO2. *Materials Chemistry and Physics*, *314*, 128909. https://doi.org/10.1016/j.matchemphys.2024.128909

Ramli, H., Zainal, N. F. A., Hess, M., & Chan, C. H. (2022). Basic principle and good practices of rheology for polymers for teachers and beginners. *Chemistry Teacher International*, *4*, 307–326. https://doi.org/10.1515/cti-2022-0010

Savić Gajić, I. M., Savić, I. M., & Svirčev, Z. (2023). Preparation and characterization of alginate hydrogels with high water-retaining capacity. *Polymers*, *15*, 2592. https://doi.org/10.3390/polym15122592

Silva, L. d. S., Vila Nova, B. G., Sousa, C. E. M. d., Silva, R. G., Carvalho, L. R. d. S., Silva, I. S. S., Moreira, P. H. d. A., Cardenas, A. F. M., Monteiro, C. d. A., Tofanello, A., Garcia, W., Teixeira, C. S., & da Silva, L. C. N. (2024). Fabrication and characterization of physically crosslinked alginate/chitosan-based hydrogel loaded with neomycin for the treatment of skin infections caused by Staphylococcus aureus. *International Journal of Biological Macromolecules*, *271*, 132577. https://doi.org/10.1016/j.ijbiomac.2024.132577

Stojkov, G., Niyazov, Z., Picchioni, F., & Bose, R. K. (2021). Relationship between structure and rheology of hydrogels for various applications. *Gels*, *7*, 255. https://doi.org/10.3390/gels7040255

Timotius, D., Kusumastuti, Y., & Rochmadi, R. (2022). Characterization and equilibrium study of drug release of ph-responsive chitosan-graft-maleic film. *International Journal of Technology*, *13*(2), 398–409. https://doi.org/10.14716/ijtech.v13i2.4594

Wang, H., Yang, J., Tian, W., Peng, K., Xue, Y., Zhao, H., Ma, X., Shi, R., & Chen, Y. (2024). A sodium alginate/carboxymethyl chitosan dual-crosslinked injectable hydrogel scaffold with tunable softness/hardness for bone regeneration. *International Journal of Biological Macromolecules*, *257*, 128700. https://doi.org/10.1016/j.ijbiomac.2023.128700

Wang, H., Yang, L., & Yang, Y. (2025). A review of sodium alginate-based hydrogels: Structure, mechanisms, applications, and perspectives. *International Journal of Biological Macromolecules*, *292*, 139151. https://doi.org/10.1016/j.ijbiomac.2024.139151

Yang, W., Chen, J., Zhao, Z., Wu, M., Gong, L., Sun, Y., Huang, C., Yan, B., & Zeng, H. (2023). Recent advances in fabricating injectable hydrogels via tunable molecular interactions for bio-applications. *Journal of Materials Chemistry B*, *12*, 332–349. https://doi.org/10.1039/d3tb02105j

Zamini, N., Mirzadeh, H., Solouk, A., & Shafipour, R. (2025). Injectable in-situ forming hydrogel based on carboxymethyl chitosan for sustained release of hyaluronic acid: A viscosupplement for biomedical applications. *Carbohydrate Polymers*, *352*, 123227. https://doi.org/10.1016/j.carbpol.2025.123227

Zhang, X., Li, Y., Ma, Z., He, D., & Li, H. (2021). Modulating degradation of sodium alginate/bioglass hydrogel for improving tissue infiltration and promoting wound healing. *Bioactive Materials*, *6*, 3692–3704. https://doi.org/10.1016/j.bioactmat.2021.03.038

Zhang, Z., & Qiao, X. (2021). Influences of cation valence on water absorbency of crosslinked carboxymethyl cellulose. *International Journal of Biological Macromolecules*, *177*, 149–156. https://doi.org/10.1016/j.ijbiomac.2021.02.080

Zhao, C., Lv, Q., & Wu, W. (2022). Application and prospects of hydrogel additive manufacturing. *Gels*, *8*, 297. https://doi.org/10.3390/gels8050297

Zhao, H., Li, J., Cong, S., Hou, H., Zhang, G., & Bi, J. (2025). Fabrication and anti-swelling properties of gelatin/sodium alginate–carboxymethyl chitosan-based cationic coordination hydrogels. *Foods*, *14*(18), 3149. https://doi.org/10.3390/foods14183149